Inorganic Chemistry

ARTICLE

pubs.acs.org/IC

Noble Reaction Features of Bromoborane in Oxidative Addition of B−Br σ-Bond to [M(PMe$_3$)$_2$] (M = Pt or Pd): Theoretical Study

Guixiang Zeng and Shigeyoshi Sakaki*

Fukui Institute for Fundamental Chemistry, Kyoto University, Takano-Nishihiraki-cho 34-4, Sakyo-ku, Kyoto 606-8103, Japan

Supporting Information

ABSTRACT: Through detailed calculations by density functional theory and second-order Møller−Plesset perturbation theory (MP2) to fourth-order Møller−Plesset perturbation theory including single, double, and quadruple excitations [MP4(SDQ)] methods, we investigated the oxidative addition of the B−Br bond of dibromo(trimethylsiloxy)borane [Br$_2$B(OSiMe$_3$)] to Pt(0) and Pd(0) complexes [M(PMe$_3$)$_2$] (M = Pt or Pd) directly yielding a trans bromoboryl complex *trans*-[MBr{BBr(OSiMe$_3$)}(PMe$_3$)$_2$]. Two reaction pathways are found for this reaction: One is a nucleophilic attack pathway which directly leads to the trans product, and the other is a stepwise reaction pathway which occurs through successive cis oxidative addition of the B−Br bond to [M(PMe$_3$)$_2$] and thermal cis−trans isomerization. In the Pt system, the former course occurs with a much smaller energy barrier (E_a = 5.8 kcal/mol) than the latter one (E_a = 20.7 kcal/mol), where the DFT-calculated E_a value is presented hereafter. In the Pd system, only the latter course is found in which the rate-determining steps is the cis−trans isomerization with the E_a of 15.1 kcal/mol. Interestingly, the thermal cis−trans isomerization occurs on the singlet potential energy surface against our expectation. This unexpected result is understood in terms of the strong donation ability of the boryl group. Detailed analyses of electronic processes in all these reaction steps as well as remarkable characteristic features of [Br$_2$B(OSiMe$_3$)] are also provided.

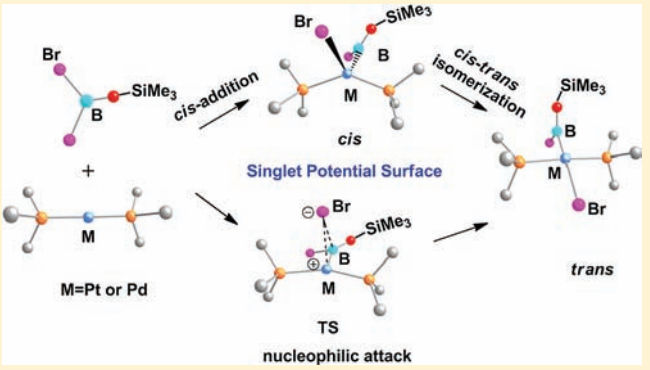

1. INTRODUCTION

The chemistry of transition-metal boryl complexes[1] has been experiencing a robust development in the past few decades due to their essential roles not only in hydroboration[2] and diboration[3] reactions of such unsaturated compounds as alkene, alkyne, aldehydes, and diene but also in the selective functionalizations of C−H[4] and C−F[5] bonds. As well-known, oxidative additions of B−H,[2] B−B,[3] and B−E (E = Si, Ge, or Sn)[6−13] bonds to low-valent transition-metal complexes are often used to prepare transition-metal boryl compounds. Usually, these oxidative additions produce cis boryl complexes.[3c,d,6,7,13,14] Interestingly, however, the oxidative addition of B−X (X = Cl, Br, or I) bond to Pd(0) and Pt(0) complexes generally affords trans boryl complexes.[15−28] Though structural properties, M−B bond nature, and catalytic reactions of transition-metal boryl complexes have been extensively investigated theoretically and experimentally,[1b−d,19,29−33] the mechanism which leads to the formation of trans boryl complexes has not been clarified yet at all. It is of considerable interest to clarify the mechanism of this new oxidative addition reaction.

In addition, the cis−trans isomerization of transition-metal complexes has received widespread interests due to their elementary importance in organometallic reactions, as recently reviewed.[34] Thermal cis−trans isomerization including spin conversion from singlet to triplet potential energy surface has been well documented.[35−37] However, the thermal cis−trans isomerization on the singlet potential energy surface has been little investigated.

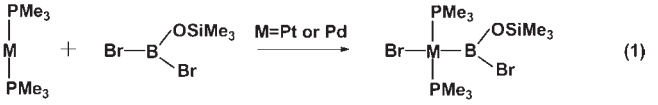

(1)

Here, we theoretically investigate the oxidative addition of bromoborane to zero-valent d^{10} Pt(0) and Pd(0) complexes, [M(PMe$_3$)$_2$] (M = Pt or Pd), as demonstrated in eq 1, where we employed dibromo(trimethylsiloxy)borane [Br$_2$B(OSiMe$_3$)] as a substrate. This is because the oxidative addition of this substrate has been proven to be a facile access to obtain trans bromoboryl complexes (Scheme 1),[15,19,20,26] and also the first stable oxoboryl complex [Pt(BO)(Br)(PCy$_3$)$_2$] (Cy = cyclohexyl) was successfully synthesized with this substrate, as recently reported by Braunschweig's group.[27] Our purposes here are to explore possible reaction pathways leading to the formation of trans bromoboryl complexes and to clarify whether the thermal cis−trans isomerization of a transition-metal complex can occur on the singlet potential energy surface or not. Through this study, we also wish to clarify interesting characteristics of [Br$_2$B(OSiMe$_3$)].

Received: April 12, 2011
Published: May 10, 2011

   dx.doi.org/10.1021/ic200749w | *Inorg. Chem.* 2011, 50, 5290–5297

Scheme 1. Synthesis of *trans*−[PtBr{BBrX}(PCy$_3$)$_2$] Through Oxidative Addition of the B−Br Bond to [Pt(PCy$_3$)$_2$] Reported by Branschweig's group[15,19,20,26,27]

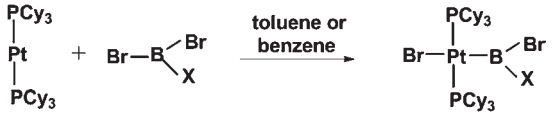

X=OSiMe$_3$, NMe$_2$, 2,4,6-Me$_3$-C$_6$H$_2$, NC$_5$H$_{10}$ etc

2. COMPUTATIONAL DETAILS

Geometries of all species were fully optimized with the density functional theory (DFT) method[38] using the B3LYP functional[39] implemented in the Gaussian 03 and 09 programs.[40] Core electrons of Pt and Pd were replaced with the effective core potentials (ECPs) LANL2DZ,[41] and their valence electrons were represented by (541/541/111/1) and (541/541/211/1) basis sets[42,43] for Pt and Pd, respectively. The 6-311+G* basis set was employed for Br and the 6-311G* basis sets were used for other atoms. Frequency calculation was carried out for each stationary point to make sure whether it is in an equilibrium structure or a transition state. The polarizable continuum model (PCM)[44]was employed to compute potential energy (E_{sol}^{pot}) and nonelectrostatic interaction energy ($\Delta E_{nonelect}$) in the solvent (toluene), where gas-phase optimized structures were employed.

Here, we provide energy (E_{sol}) with zero-point energy correction as well as the Gibbs energy (G_{sol}^0) in solvent to discuss the reaction profile. For each species, the E_{sol} is defined through eq 2:

$$E_{sol} = E_{sol}^{pot} + E_{nonelect} + E_{gas}^{v_0} \quad (2)$$

where $E_{gas}^{v_0}$ represents the zero-point vibrational energy in the gas phase. In a bimolecular process, such as the coordination of the substrate [Br$_2$B(OSiMe$_3$)] with [M(PMe$_3$)$_2$], the entropy change must be taken into consideration because the entropy considerably decreases in the process. In this case, Gibbs energy (G_{sol}^0) must be evaluated as follows:

$$\begin{aligned} G_{sol}^0 &= H^0 - T(S_r^0 + S_v^0 + S_t^0) \\ &= E^T + P\Delta V - T(S_r^0 + S_v^0 + S_t^0) \\ &= E_{sol} + E_{therm} - T(S_r^0 + S_v^0 + S_t^0) \end{aligned} \quad (3)$$

where ΔV is 0 in solution, E_{therm} is the thermal correction by translational, vibrational, and rotational movements, S_r^0, S_v^0, and S_t^0 are rotational, vibrational, and translational entropies, respectively. In general, the Thacker−Ttrode equation is used to evaluate translational entropy S_t^0. In solution phase, however, the usual Sackur−Tetrode equation cannot be directly applied to the evaluation of S_t^0, because S_t^0 is suppressed very much in solution.[45] In this context, we evaluated the translational entropy with the method developed by Whitesides et al.[46]

3. RESULTS AND DISCUSSION

In the first three subsections, geometry and energy changes in the oxidative addition of the B−Br bond of [Br$_2$B(OSiMe$_3$)] to [M(PMe$_3$)$_2$] (M=Pt or Pd) are explored. Two possible reaction pathways and their electronic processes as well as remarkable features of [Br$_2$B(OSiMe$_3$)] are discussed. One is a nucleophilic attack pathway in which the bromoborane undergoes the nucleophilic attack of Pt(PMe$_3$)$_2$ to directly form a trans product *trans*-[MBr{BBr(OSiMe$_3$)}(PMe$_3$)$_2$], and the other is a stepwise reaction pathway which occurs through cis oxidative addition followed by cis−trans isomerization. All reactions are found to occur on the singlet potential energy surface. This phenomenon is unexpected for the thermal cis−trans isomerization process of a planar four-coordinate d^8 transition-metal complex. In the fourth subsection, we present clear explanation on this unexpected phenomenon. At last, we wish to elucidate in which case the trans product is directly formed through the nucleophilic attack pathway and in which case it is formed through the stepwise pathway including the cis−trans isomerization.

3.1. Geometry and Energy Changes in Platinum Reaction System Yielding the trans Bromoboryl Complex, *trans*-[PtBr{BBr(OSiMe$_3$)}(PMe$_3$)$_2$]. Optimized geometries and energy changes along two reaction pathways are shown in Figure 1. In [Pt(PMe$_3$)$_2$] **1**−**Pt**, the Pt−P distance is 2.266 Å, and the P−Pt−P moiety is almost linear. [Br$_2$B(OSiMe$_3$)] **2** is planar, in which the B−Br bond distance is 1.955 Å. The first step is the coordination of **2** with **1**−**Pt** to form a precursor complex [Pt(PMe$_3$)$_2$-{Br$_2$B(OSiMe$_3$)}] **3**−**Pt** through the interaction between the empty p orbital of B and the doubly occupied d$_\sigma$ orbital of Pt, which will be discussed below. Thus, **3**−**Pt** can be considered as a Lewis acid−base adduct. This process occurs through a transition-state **TS$_{1,3}$**−**Pt** with moderate activation energy of 7.1/16.4 kcal/mol and a reaction energy of −3.8/6.7 kcal/mol, where we provide both the energy change (E_{sol}) and Gibbs energy change (G_{sol}^0) before and after slash, respectively. In **TS$_{1,3}$**−**Pt**, the Pt−B distance is 3.132 Å, suggesting that the interaction between Pt and B is weak. In consistent with the long Pt−B distance, two B−Br bonds are only slightly elongated by 0.032 and 0.013 Å. In **3**−**Pt**, the Pt−B bond is shortened to 2.178 Å, suggesting that a strong interaction is formed between Pt and B. As a result, B−Br1 and B−Br2 bonds are somewhat elongated by 0.124 and 0.119 Å, respectively (see Figure 1 for Br1 and Br2).

Similar complexes of [Pt(PR$_3$)$_2$] with Lewis acids were reported experimentally,[47] and some of them were theoretically investigated previously.[48] In the case of GaBr$_3$, such a complex is not formed, but the Ga−Br bond undergoes oxidative addition to [Pt(PR$_3$)$_2$] to form *trans*-[Pt(Br)(GaBr$_2$)(PR$_3$)$_2$], like bromoborane.[47c] All these interestingly relate to the present work.

Starting from **3**−**Pt**, there are two pathways leading to a final trans form of platinum(II) bromoboryl complex *trans*-[PtBr-{BBr(OSiMe$_3$)}(PMe$_3$)$_2$] **5**−**Pt**. One is the nucleophilic attack pathway which directly provides **5**−**Pt**, and another is the stepwise pathway which occurs through the cis oxidative addition to form a cis intermediate *cis*-[PtBr{BBr(OSiMe$_3$)}(PMe$_3$)$_2$] **4**−**Pt** and its subsequent isomerization to **5**−**Pt**.

In the nucleophilic attack pathway, **5**−**Pt** is directly produced through a transition-state **TS$_{3,5}$**−**Pt**, as shown in the lower part of Figure 1. In **TS$_{3,5}$**−**Pt**, the B−Br1 and Pt−Br1 distances are 3.005 and 2.974 Å, respectively. These data indicate that the B−Br1 is almost broken, but the Pt−Br1 bond is far from the formation. The activation barrier for this step is 5.8/5.9 (12.6) kcal/mol, where the activation barrier is defined as an energy difference between the transition state and the intermediate just before the transition state; in parentheses is the energy difference between the transition state and the sum of reactants, hereafter. Note that the true activation barrier is the energy difference between the transition state and the sum of reactants when the intermediate is less stable than the sum of reactants. To verify this transition state, we performed an intrinsic reaction coordinate (IRC) calculation in solvent. But, it stopped at a structure corresponding to an ion pair, in which the B−Br1 and Pt−Br1 distances are further elongated to 3.473 and 3.322 Å, respectively (see Figure 1). These geometrical features suggest that the Br$^-$ anion would easily dissociate from the system. To investigate whether the Br$^-$ anion easily dissociates or not, we calculated the dissociation energy, which is defined as an energy

dx.doi.org/10.1021/ic200749w |*Inorg. Chem.* 2011, 50, 5290–5297

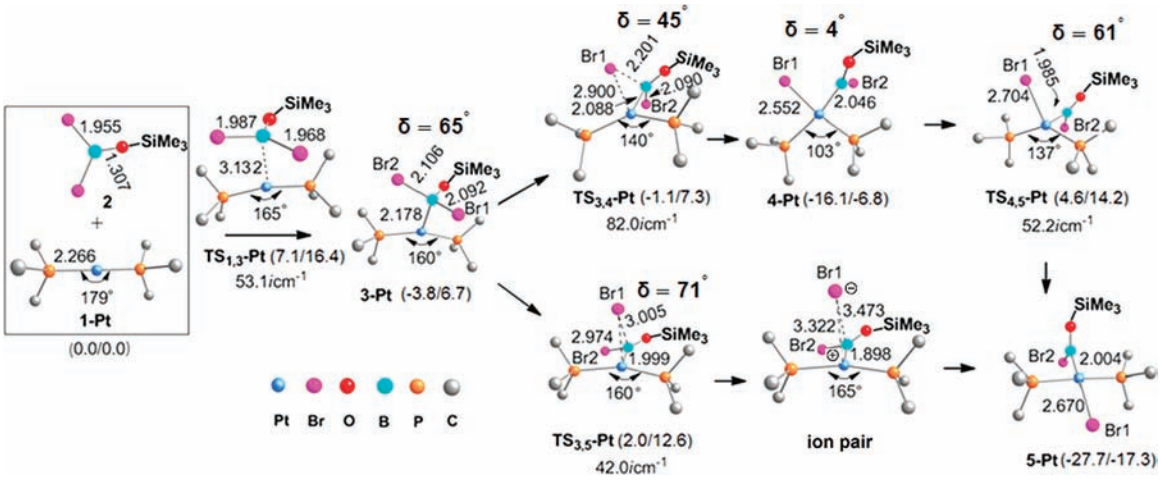

Figure 1. Optimized structures of all species involved in the formation reaction of *trans*-[PtBr{BBr(OSiMe$_3$)}(PMe$_3$)$_2$]. All the hydrogen atoms are omitted for clarity. All the distances and angles are in Å and °, respectively. Free energy change E_{sol} and Gibbs energy change ΔG^0_{sol} are shown before and after the slash, respectively, in kcal/mol unit. The standard (energy zero) is the sum of [Pt(PMe$_3$)$_2$]and [Br$_2$B(OSiMe$_3$)].

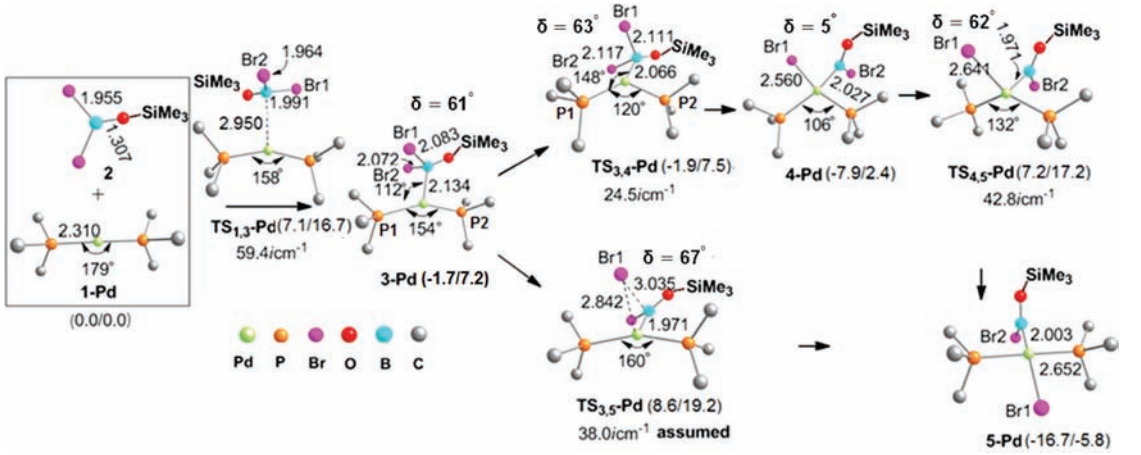

Figure 2. Optimized structures of all the species involved in the formation reaction of *trans*-[PdBr{BBr(OSiMe$_3$)}(PMe$_3$)$_2$]. All the hydrogen atoms are omitted for clarity. All the distances and angles are in Å and °, respectively. Free energy change E_{sol} and Gibbs energy change ΔG^0_{sol} are shown before and after the slash, respectively, in kcal/mol unit. The standard (energy zero) is the sum of [Pd(PMe$_3$)$_2$] and [Br$_2$BOSiMe$_3$].

difference between **3**−**Pt** and the sum of separate Br^- anion and $[Pt(\mathbf{B})(PMe_3)_2]^+$ cation in solvent, where the [BBr(OSiMe$_3$)] ligand is represented by (**B**) for brevity hereafter. The dissociation energy is 30.4 kcal/mol, which is much larger than the activation barrier for **TS$_{3,5}$**−**Pt**. This indicates that the Br^- does not completely dissociate from the Pt cation but stays around the Pt cation as a counteranion to form the ion pair due to the Coulomb interaction. Note that toluene is not polar enough to stabilize the separate cation and anion. Actually, the approximate potential energy surface scan starting from the ion pair clearly demonstrates that the Br^- anion moves around the Pt cation toward the position trans to the (**B**) ligand (see Figure S1, Supporting Information for details). This movement of the Br^- anion and its coordination with the Pt center occurs without any barrier. Based on these results, it is concluded that **TS$_{3,5}$**−**Pt** is the correct transition state leading to the final trans product **5**−**Pt**. Nucleophilic attack of Pt(0) complex to organic halide was theoretically investigated by Ziegler[49] and our groups[50] previously, but it has not been clarified how much easier the rebound process of the anion at the trans position occurs. This reaction mechanism is completely different from the mechanism yielding the cis product by the cis oxidative addition reaction.

In the stepwise pathway, the first step is the cis oxidative addition. This step occurs through a transition-state **TS$_{3,4}$**−**Pt** to form a cis intermediate **4**−**Pt**, as shown in the upper part of Figure 1. In **TS$_{3,4}$**−**Pt**, the B−Br1 bond is elongated to 2.201 Å, while the B−Br2 bond distance is little changed. In consistent with the elongation of the B−Br1 bond, the Pt−B bond becomes short to 2.088 Å, indicating that the Pt−B bond is almost formed in **TS$_{3,4}$**−**Pt**. In **4**−**Pt**, the Pt−Br1 (2.252 Å) bond as well as the Pt−B (2.046 Å) bond is formed. During this process, the P−Pt−P angle decreases from 160° in **3**−**Pt** to 140° in **TS$_{3,4}$**−**Pt** and 103° in **4**−**Pt**. At the same time, the dihedral angle between the P−Pt−P and B−Pt−Br1 planes decreases from 65° in **3**−**Pt** to 45° in **TS$_{3,4}$**−**Pt** and 4° in **4**−**Pt**. The almost planar structure of **4**−**Pt** is consistent with our general understanding that the d^8 transition-metal complex tends to take a four-coordinate planar structure in the singlet state. This step occurs with a considerably large exothermicity of

dx.doi.org/10.1021/ic200749w |*Inorg. Chem.* 2011, 50, 5290–5297

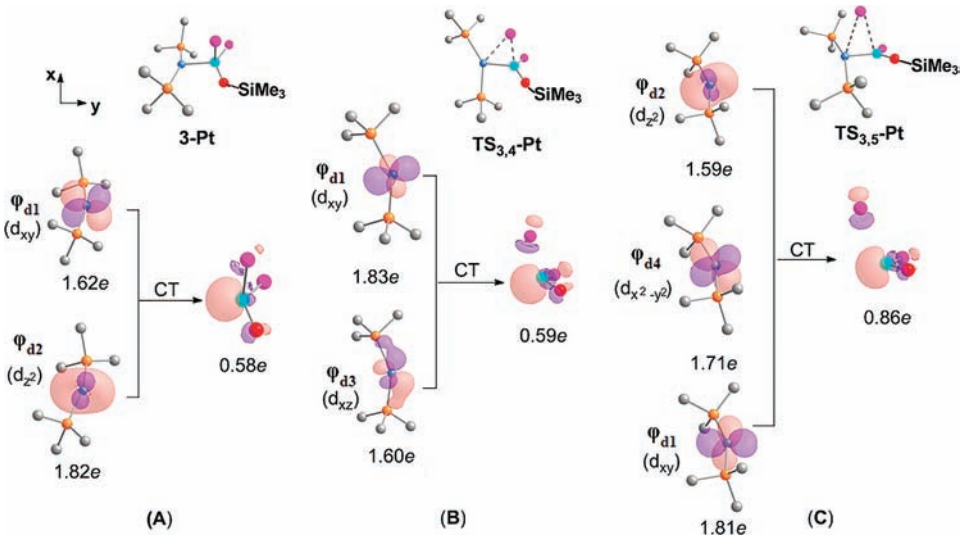

Figure 3. Electron populations of MOs of fragments, $[Pt(PMe_3)_2]$ and $[Br_2B(OSiMe_3)]$.

12.3/13.5 kcal/mol and a very small energy barrier of 2.7/0.6 (7.3) kcal/mol. These results indicate that the cis intermediate is easily formed. The next step is the cis−trans isomerization to the final trans product **5**−**Pt** through a transition-state **TS$_{4,5}$**−**Pt**. In **TS$_{4,5}$**−**Pt**, the P−Pt−P angle is considerably increases to 137°. The Pt−Br1 bond is elongated to 2.704 Å. On the other hand, the Pt−B bond is moderately shortened to 1.985 Å. The dihedral angle δ is 61°, indicating that this transition state is pseudotetrahedral. Generally, the d^8 transition-metal complex takes a triplet ground state in a tetrahedral-like structure. However, **TS$_{4,5}$**−**Pt** takes a singlet ground state despite of its pseudotetrahedral geometry, which will be discussed in Section 3.4 in more detail. This transformation occurs with activation barrier of 20.7/21.0 kcal/mol and exothermicity of 11.6/10.5 kcal/mol.

In summary, the overall reaction is exothermic by 27.7/17.3 kcal/mol. In the nucleophilic attack pathway, the activation barrier is 5.8/5.9 (12.6) kcal/mol. In the stepwise approach, the rate-determining step is the cis−trans isomerization with the activation barrier of 20.7/21.0 kcal/mol. Thus, the nucleophilic attack pathway is much more favorable than the stepwise one.

3.2. Geometry and Energy Changes in Palladium Reaction System Yielding trans Bromoboryl Complex, *trans*-[PdBr{BBr(OSiMe$_3$)}(PMe$_3$)$_2$]. Optimized geometries and energy changes of all stationary points are shown in Figure 2. In this oxidative addition, only the stepwise pathway was found. The transition state for the nucleophilic attack pathway could not be located. However, for the purpose of comparison, this reaction course is also discussed below.

The first step is the coordination of **2** with $[Pd(PMe_3)_2]$ **1**−**Pd** to form a precursor complex $[Pd(PMe_3)_2\{Br_2B(OSiMe_3)\}]$ **3**−**Pd**. This process occurs through a transition-state **TS$_{1,3}$**−**Pd**. In **TS$_{1,3}$**−**Pd**, the Pd−B distance (2.950 Å) is somewhat shorter than that in **TS$_{1,3}$**−**Pt** (3.132 Å). The activation barrier of this step is 7.1/16.7 kcal/mol, and the reaction energy is −1.7/7.2 kcal/mol. Then, **3**−**Pd** transforms to a cis intermediate *cis*-$[PdBr(PMe_3)_2\{BrB(OSiMe_3)\}]$ **4**−**Pd** through the second transition-state **TS$_{3,4}$**−**Pd**. This process is the cis oxidative addition. When going from **3**−**Pd** to **TS$_{3,4}$**−**Pd**, the Pd−B distance becomes somewhat shorter by 0.068 Å, and the B−Br1 and B−Br2 bonds are moderately elongated by 0.028 and 0.045 Å, respectively. The P1−Pd−P2 angle considerably decreases by 34°, and the P1−Pd−B angle considerably increases by 36°. These angle changes necessarily occur to generate the cis intermediate **4**−**Pd**. The activation barrier and the reaction energy for this step are 0.2/0.3(7.5) kcal/mol and −6.2/−4.8 kcal/mol, respectively, indicating that this step easily occurs. Finally, **4**−**Pd** transforms to a trans product *trans*-[PdBr{BBr(OSiMe$_3$)}(PMe$_3$)$_2$] **5**−**Pd** through a pseudotetrahedral transition-state **TS$_{4,5}$**−**Pd** on the singlet potential energy surface. In **TS$_{4,5}$**−**Pd**, the dihedral angle δ between the P−M−P and B−M−Br1 planes is 62°. The activation barrier and the reaction energy for this step are 15.1/14.8 and 8.8/8.2 kcal/mol, respectively, indicating that the cis−trans isomerization is the rate-determining step, like in the Pt reaction system.

In the nucleophilic attack pathway, the transition state could be optimized only when the P−Pd−P angle was fixed to be 160°, which is the same as that in **TS$_{3,5}$**−**Pt**. This constrained transition-state **TS$_{3,5}$**−**Pd** lies moderately higher in energy than **TS$_{4,5}$**−**Pd** by 1.4/2.0 kcal/mol.[51] Despite of this small energy difference, **TS$_{3,5}$**−**Pd** eventually changes to **TS$_{4,5}$**−**Pd** during the geometry optimization without the constraint of the P−Pd−P angle. This will be discussed below in more detail. These results indicate that the nucleophilic attack pathway is unlikely.

In summary, the oxidative addition of the B−Br σ-bond to $[Pd(PMe_3)_2]$ occurs in the stepwise pathway, the rate-determining step of which is the cis−trans isomerization step. The nucleophilic attack pathway is unlikely, on the other hand, the reason of which will be discussed below.

3.3. Electronic Process of the Oxidative Addition of B−Br Bond. First, we investigate the population changes in the oxidative addition of the B−Br bond, to clarify the electronic process. As well-known, the molecular orbital (MO) of a total system AB can be represented by a linear combination of MOs of fragments, A and B, as follows:

$$\phi_i(\mathrm{AB}) = \sum_m C_{im}^{\mathrm{A}}\phi_m(\mathrm{A}) + \sum_n C_{in}^{\mathrm{B}}\phi_n(\mathrm{B}) \qquad (4)$$

where φ_i(AB) represents the i-th MO of the complex AB, φ_m(A) and φ_n(B) are the m-th MO and n-th MO of fragments A and B, respectively, and C_{im}^{A} and C_{in}^{B} are the expansion coefficients of

dx.doi.org/10.1021/ic200749w |*Inorg. Chem.* 2011, 50, 5290–5297

Scheme 2. Schematic Picture of the B−Br σ^* MO of $[Br_2B(OSiMe_3)]$

Table 1. Relative Stability of Singlet and Triplet States Calculated with Various Methods[a]

	$TS_{4,5}$−Pt	$TS_{4,5}$−Pd	TS−Br_2
MP2	3.06	2.86	−0.51
MP3	2.33	2.03	−0.16
MP4(DQ)	2.69	2.48	−0.34
MP4(SDQ)	2.74	2.55	−0.39
SCS-MP2	2.51	2.79	−0.54
B3LYP	1.93	2.0	−0.23
B3PW91	1.92	1.98	−0.21
BLYP	1.87	1.93	−0.27
PBEPBE	1.86	1.92	−0.25

[a] A positive value represents that the singlet state is more stable than the triplet state. Values given in eV units.

φ_m(A) and φ_n(B), respectively. The Mulliken populations of φ_m(A) and φ_n(B) can be obtained from these coefficients C^A_{im} and C^B_{in}. Here, we separate the total system into $[M(PMe_3)_2]$ and $[Br_2B(OSiMe_3)]$ **2**. In the precursor complex **3**−**Pt**, the electron population mainly decreases in φ_{d1} and φ_{d2} of $[Pt(PMe_3)_2]$ by 0.38*e* and 0.18*e*, respectively, where the φ_{d1} and φ_{d2} mainly consist of d_{xy} and d_{z^2} orbitals of Pt, respectively, as shown in Figure 3A. On the other hand, the electron population increases in the empty p orbital ϕ_1 of **2** by 0.58*e*. These population changes clearly show that the charge transfer (CT) mainly occurs from the φ_{d1} and φ_{d2} of $[Pt(PMe_3)_2]$ to the empty p orbital of **2** in **3**−**Pt**. In the transition-state $\mathbf{TS_{3,4}}$−**Pt** of the cis oxidative addition, the CT (0.57*e*) occurs from the φ_{d2} and φ_{d3} of $[Pt(PMe_3)_2]$ to the σ^*-like MO ϕ_2 of **2**; see Figure 3B, where φ_{d3} mainly consists of d_{xz}. This ϕ_2 mainly consists of the sp^2 orbital of the B atom into which the p_σ orbital of the Br atom mixes in an antibonding way, as will be discussed below. This is one important feature of the borane substrate. This CT induces the B−Br bond weakening and simultaneously the increase in the oxidation state of Pt. In the transition state $\mathbf{TS_{3,5}}$−**Pt** of the nucleophilic attack pathway, the similar CT (0.89*e*) occurs from φ_{d1}, φ_{d2}, and φ_{d4} orbitals of $[Pt(PMe_3)_2]$ to the ϕ_3 of **2**, where the φ_{d4} mainly consists of $d_{x^2-y^2}$ (see Figure 3C). This CT is much larger than that in $\mathbf{TS_{3,4}}$−**Pt**. The acceptor orbital ϕ_3 is similar to the ϕ_2 of $\mathbf{TS_{3,4}}$−**Pt**. As a result, the B−Br bond is more weakened by this CT in $\mathbf{TS_{3,5}}$−**Pt**, which is evidenced by the considerable elongation (0.913 Å) of the B−Br bond.

It should be noted that the ϕ_2 and ϕ_3 are the antibonding MO between the sp^2 orbital of the B atom and the p_σ orbital of the Br atom, and they apparently expand toward the Pt atom (see ϕ_2 and ϕ_3 in Figure 3). This orbital expansion enhances the orbital overlap with the d orbitals of Pt, which is favorable for the oxidative addition. Thus, it is interesting to clarify the reason why the ϕ_2 and ϕ_3 expand toward the Pt atom. In $[Br_2B(OSiMe_3)]$, the B atom possesses an empty p orbital perpendicular to the

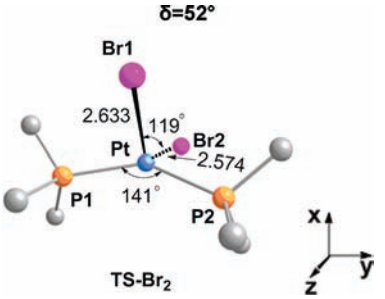

Figure 4. Transition state for the cis−trans isomerization of $[PtBr_2(PMe_3)_2]$.

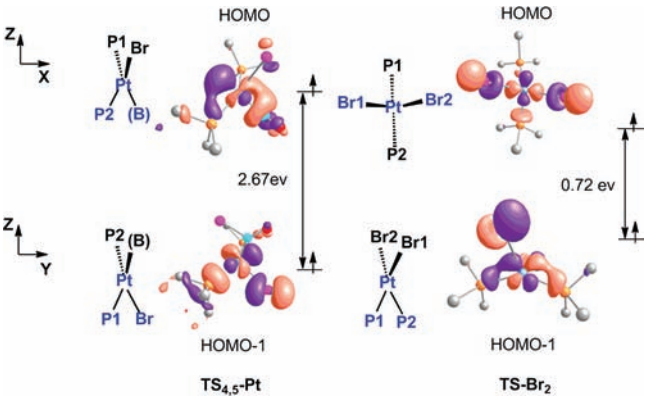

Figure 5. The d−d orbital splitting in $\mathbf{TS_{4,5}}$−**Pt** and TS−$\mathbf{Br_2}$. Unrestricted DFT calculations were carried out for the triplet state, where the singlet optimized geometry of $\mathbf{TS_{4,5}}$−**Pt** was employed. For TS−$\mathbf{Br_2}$, the triplet optimized geometry was employed, because the triplet state is more stable than the closed-shell singlet state. (**B**) = $[BBr(OSiMe_3)]$, and P1 = P2 = $[PMe_3]$.

molecular plane. Because this empty p orbital lies in higher energy than the p_σ orbital of the Br atom, it mixes into the sp^2 orbital on the B atom in a bonding way with the Br p_σ orbital. This mixing changes the direction of the B−Br σ^* MO toward the Pt atom, as shown in Scheme 2.

In **3**−**Pd** and $\mathbf{TS_{3,4}}$−**Pd**, the similar CT processes are found. However, the total amount of CT is smaller than that in the Pt system. For instance, the CT from the $[M(PMe_3)_2]$ moiety to the **2** moiety is 0.40*e* and 0.56*e* in **3**−**Pd** and **3**−**Pt**, respectively, 0.51*e* and 0.57*e* in $\mathbf{TS_{3,4}}$−**Pd** and $\mathbf{TS_{3,4}}$−**Pt**, and 0.78*e* and 0.89*e* in $\mathbf{TS_{3,5}}$−**Pd** and $\mathbf{TS_{3,5}}$−**Pt**. The small CTs of the Pd reaction system arise from the fact that the d orbital energy is lower in the Pd system than in the Pt system, as is well-known[52] (see also the Figure S4, Supporting Information).

3.4. Why Does the cis−trans Isomerization Occur on the Singlet Potential Energy Surface? The isomerization of the cis intermediate (**4**−**Pt** and **4**−**Pd**) to the trans form has been proved here to unexpectedly occur on the singlet potential energy surface without spin conversion, as mentioned in Sections 3.1 and 3.2. This is another important and interesting feature of the reaction of bromoborane, because it is believed in general that the thermal cis−trans isomerization of d^8 four-coordinate planar transition-metal complex occurs through spin conversion from singlet to triplet. Here, we recalculated the relative stabilities of the singlet and triplet states with various methods, because the relative stability between these two states is sensitive to the

dx.doi.org/10.1021/ic200749w |*Inorg. Chem.* 2011, 50, 5290–5297

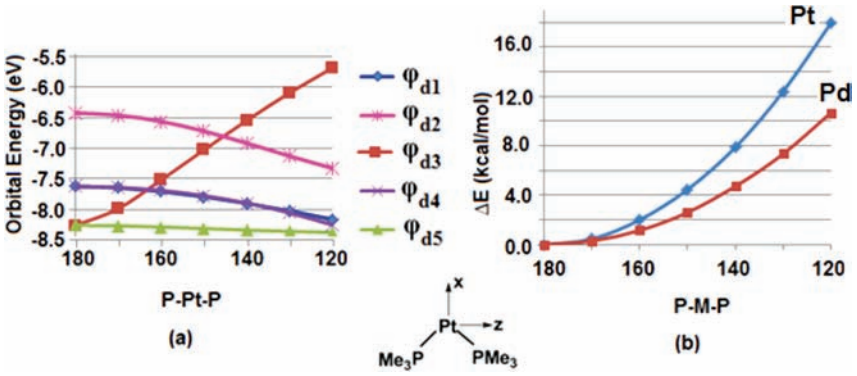

Figure 6. Total energy and the orbital energy changes against the P−Pt−P angle (in °).

computational method. All these computational results indicate that the singlet state is considerably more stable than the triplet state, as shown in Table 1. Moreover, all computational methods provide similar energy difference between the singlet and the triplet states (1.9 to 2.8 eV). These results lead to the conclusion that the cis−trans isomerization occurs on the singlet potential energy surface.

It is of considerable importance to provide a clear explanation for this unexpected transition state on the singlet potential energy surface. To make comparisons with the typical cis−trans isomerization, we investigated the cis−trans isomerization of *cis*-$[PtBr_2(PMe_3)_2]$. The transition-state **TS−Br$_2$** is pseudotetrahedral, as shown in Figure 4. In **TS−Br$_2$**, the Pt−Br1 and Pt−Br2 distances are 2.633 and 2.574 Å, respectively. The Br−Pt−Br angle is 119°, which exists almost on the *xy* plane. The P−Pt−P angle is 141°, which exists almost on the *yz* plane (see Figure 4 for *x*, *y*, and *z* axes). As a result, d_{xy} and d_{yz} orbitals are destabilized by two bromide and two phosphine ligands, respectively. The energy gap between these two d orbitals is 0.72 eV, as shown in Figure 5, where the Kohn−Sham orbital energies are presented. Due to this small energy splitting, the triplet state becomes more stable than the singlet for **TS−Br$_2$**, as shown in Table 1.

In **TS$_{4,5}$−Pt**, on the other hand, one bromide ligand is substituted for the boryl group (B). The boryl and one phosphine ligand exist on the *xy* plane with the P1−Pt−B angle of 88°. Thus, the d_{xy} orbital energy is considerably destabilized by these two ligands. The bromide and the other phosphine ligands lie on the *xz* plane with the P2−Pt−Br angle of 89°, which destabilize the d_{xz} orbital energy. The energy gap between these two d orbitals is 2.67 eV, which is much larger than that of **TS−Br$_2$** (see Figure 5). Similarly, the d−d splitting energy is 2.75 eV in **TS$_{4,5}$−Pd** (see Figure S3, Supporting Information). These large d−d energy splittings arise from the strong donating ability of the boryl ligand, as follows: The highest occupied molecular orbital (HOMO) energy of the boryl ligand is much higher than that of the Br ligand by 2.2 eV. In other words, the boryl ligand is much stronger than the bromide ligand. For the presence of the HOMO at high energy, the boryl ligand considerably raises the d_{xy} orbital energy, leading to the large d−d energy splitting. Thus, the singlet state is more stable than the triplet one even in the pseudotetrahedral **TS$_{4,5}$−Pt** and **TS$_{4,5}$−Pd**.

In summary, one d orbital is extremely destabilized by the strong boryl ligand in the transition state of the cis−trans isomerization of **4−Pt** and **4−Pd**. This is the reason why the singlet state is more stable than the triplet one even in the pseudotetrahedral transition state of the isomerization reaction.

3.5. Why Is the Nucleophilic Attack Pathway Possible in the Pt System but Not in the Pd? Another important result here is that the nucleophilic attack pathway is possible only in the Pt reaction system and not in the Pd. To get an answer to this question, we examined first the major differences between transition states for the nucleophilic attack pathway (**TS$_{3,5}$−Pt**) and the cis oxidative addition (**TS$_{3,4}$−Pt** and **TS$_{3,4}$−Pd**). The P−Pt−P angle (160°) of **TS$_{3,5}$−Pt** is much larger than those of **TS$_{3,4}$−Pt** (140°) and **TS$_{3,4}$−Pd** (120°). In addition, the electronic process is different between these two pathways, as discussed in Section 3.3. In **TS$_{3,5}$−Pt**, the CT mainly occurs from the d_σ-like MOs (φ_{d2} and φ_{d4}) of $[Pt(PMe_3)_2]$ to the B−Br σ^* MO ϕ_3, as shown in Figure 3. In **TS$_{3,4}$−Pt** and **TS$_{3,4}$−Pd**, the CT mainly occurs from the d_π-type MO φ_{d3} of $[M(PMe_3)_2]$ to the B−Br σ^* MO ϕ_2. As clearly shown in Figure 6a, the φ_{d3} orbital energy becomes higher by the bending of the P−M−P angle. Thus, the small P−M−P angle is favorable for the transition state of the cis oxidative addition, because the CT from the φ_{d3} of $[M(PMe_3)_2]$ to the B−Br σ^* orbital is crucial in the cis oxidative addition. In contrast, φ_{d2} and φ_{d4} MOs become moderately lower in energy, as the P−M−P angle decreases; see Figure 6a. This indicates that the CT from these φ_{d2} and φ_{d4} MOs of $[M(PMe_3)_2]$ to the σ^*-type ϕ_2 MO of **2** becomes weak in the small P−M−P angle. Thus, the large P−M−P angle is favorable for the nucleophilic attack pathway.

We also examined how much easier the P−M−P angle decreases. For instance, when the P−Pt−P angle decreases from 180° to 120°, the destabilization energy (ΔE) is 18.0 kcal/mol for the Pt system and 10.7 kcal/mol for the Pd system, as shown in Figure 6b. These results indicate that the P−M−P bending occurs with more difficulty in $[Pt(PMe_3)_2]$ than in $[Pd(PMe_3)_2]$. In other words, the $[Pt(PMe_3)_2]$ moiety tends to keep its linear structure, and hence the nucleophilic attack is favorable in the Pt system. In the Pd system, the cis oxidative addition becomes favorable because the P−Pd−P angle easily decreases with smaller destabilization energy. Actually, the P−Pd−P angle is smaller than the P−Pt−P angle in both the borane precursor complex **3** and the transition-state **TS$_{3,4}$** for the cis oxidative addition step (see Figures 1 and 2).

4. CONCLUSIONS

We have theoretically investigated the oxidative addition reaction of the B−Br bond of $[Br_2B(OSiMe_3)]$ **2** to $[M(PMe_3)_2]$ **1** (M = Pt or Pd) yielding the trans bromoboryl complex *trans*-$[MBr\{BBr(OSiMe_3)\}(PMe_3)_2]$. These oxidative addition reactions are thermodynamically favorable; the exothermicity is 27.7/17.3 kcal/mol

dx.doi.org/10.1021/ic200749w |*Inorg. Chem.* 2011, 50, 5290–5297

for the Pt system and 16.7/5.8 kcal/mol for the Pd system. The first step of the reaction is the coordination of **2** with **1** to form a precursor complex. The next step is the B−Br bond cleavage, in which two reaction pathways are possible: One is the nucleophilic attack pathway, and the other is the stepwise reaction pathway. In the former pathway, the final trans bromoboryl complex is directly formed through the dissociation of the Br^- anion from the B atom and its successive coordination with the metal center at the position trans to the (**B**) ligand. It is noted here that during this reaction step, the Br^- anion does not completely dissociate from the $[Pt(PMe_3)_2\{BBr(SiMe_3)\}]^+$ cation but stays around it to form an ion pair. In the latter pathway, the cis oxidative addition of the B−Br bond to the metal center forms a cis intermediate, and then it transforms to the trans product through a thermal cis−trans isomerization. For the Pt system, these two reaction courses are found, and the former one is more favorable than the latter one. For the Pd system, only the latter one is found, where the rate-determining step is the cis−trans isomerization. In both reaction courses, the empty p orbital of the B atom plays a crucial role to expand the B−Br σ^* MO toward the metal center, which is favorable for the B−Br bond cleavage.

Interestingly, the thermal cis−trans isomerization is found to occur on the singlet potential energy surface without spin conversion. In the transition state, one d orbital is much destabilized in energy by the strong (**B**) ligand. As a result, the singlet state is more stable even for the tetrahedral-like transition-states $\mathbf{TS_{4,5}}$**−Pt** and $\mathbf{TS_{4,5}}$**−Pd**. This is the first theoretical report to show that the thermal cis−trans isomerization occurs on the singlet potential surface and the reason why.

In summary, we successfully elucidated the reaction mechanism of the oxidative addition of bromoborane directly yielding the trans product, the reason why, and the mechanism of cis−trans isomerization of four-coordinate d^8 metal complex on the singlet potential surface.

■ ASSOCIATED CONTENT

Ⓢ Supporting Information. Potential, zero-point, and Gibbs free energies and Cartesian coordinates of all stationary points in this work. This material is available free of charge via the Internet at http://pubs.acs.org.

■ AUTHOR INFORMATION

Corresponding Author
*E-mail: sakaki@moleng.kyoto-u.ac.jp.

■ ACKNOWLEDGMENT

This work is financially supported by the Grant-in-Aids from Ministry of Education, Culture, Science, Sport, and Technology through Grant-in-Aids of Specially Promoted Science and Technology (no. 22000009) and Grand Challenge Project (IMS). We are also thankful to the computational facility at the Institute of Molecular Science, Okazaki, Japan.

■ REFERENCES

(1) (a) Hartwig, J. F.; Waltz, K. M.; Muhoro, C. N.; He, X.; Eisenstein, O.; Bosque, R.; Maseras, F. *Advances of Boron Chemistry*; Siebert, W., Ed.; special publication no. 201; The Royal Society of Chemistry: Cambridge, U.K., 1997; p 373. (b) Braunschweig, H.; Colling, M. *Coord. Chem. Rev.* **2001**, *223*, 1. (c) Irvine, G. J.; Lesley, M. J. G.; Marder, T. B.; Norman, N. C.; Rice, C. R.; Robins, E. G.; Roper, W. R.; Whittell, G. R.; Wright, L. J. *Chem. Rev.* **1998**, *98*, 2685. (d) Aldridge, S.; Coombs, D. L. *Coord. Chem. Rev.* **2004**, *248*, 535. (e) Pandey, K. K. *Coord. Chem. Rev.* **2009**, *253*, 37. (f) Braunschweig, H.; Dewhurst, R. D.; Schneider, A. *Chem. Rev.* **2010**, *110*, 3924.

(2) (a) Männig, D.; Nöth, H. *Angew. Chem., Int. Ed. Engl.* **1985**, *24*, 878. (b) Burgess, K.; Ohlmeyer, M. J. *Chem. Rev.* **1991**, *91*, 1179. (c) Wadepohl, H. *Angew. Chem., Int. Ed. Engl.* **1997**, *36*, 2441. (d) Beletskaya, I.; Pelter, A. *Tetrahedron* **1997**, *53*, 4957. (g) Caballero, A.; Sabo-Etienne, S. *Organometallics* **2007**, *26*, 1191. (h) Crudden, C. M.; Glasspoole, B. W.; Lata, C. J. *Chem. Commun.* **2009**, 6704. (i) Mazet, C.; Gérard, D. *Chem. Commun.* **2011**, 298.

(3) (a) Marder, T. B.; Norman, N. C. *Top. Catal.* **1998**, *5*, 63. (b) Ishiyama, T.; Matsuda, N.; Miyaura, N.; Suzuki, A. *J. Am. Chem. Soc.* **1993**, *115*, 11018. (c) Iverson, C. N.; Smith, M. R., III *J. Am. Chem. Soc.* **1995**, *117*, 4403. (d) Iverson, C. N.; Smith, M. R., III *Organometallics* **1996**, *15*, 5155. (e) Braunschweig, H.; Kupfer, T.; Lutz, M.; Radacki, K.; Seeler, F.; Sigritz, R. *Angew. Chem., Int. Ed.* **2006**, *45*, 8048. (f) Burks, H. E.; Liu, S.; Morken, J. P. *J. Am. Chem. Soc.* **2007**, *129*, 8766. (g) Braunschweig, H.; Kupfer, T. *J. Am. Chem. Soc.* **2008**, *130*, 4242. (h) Laitar, D. S.; Tsui, E. Y.; Sadighi, J. P. *J. Am. Chem. Soc.* **2006**, *128*, 11036. (i) Iwadate, N.; Suginome, M. *J. Am. Chem. Soc.* **2010**, *132*, 2548. (j) Kliman, L. T.; Mlynarski, S. N.; Morken, J. P. *J. Am. Chem. Soc.* **2009**, *131*, 13210.

(4) (a) Chen, H.; Schlecht, S.; Semple, T. C.; Hartwig, J. F. *Science* **2000**, *287*, 1995. (b) Cho, J.; Tse, M. K.; Holmes, D.; Maleczka, R. E., Jr.; Smith, M. R., III *Science* **2002**, *295*, 305. (c) Ishiyama, T.; Miyaura, N. *J. Organomet. Chem.* **2003**, *680*, 3. (d) Liskey, C. W.; Wei, C. S.; Pahls, D. R.; Hartwig, J. F. *Chem. Commun.* **2009**, 5603. (e) Hartwig, J. F. *Nature* **2008**, *455*, 314. (f) Mkhalid, I. A. I.; Coventry, D. N.; Albesa-Jove, D.; Batsanov, A. S.; Howard, J. A. K.; Perutz, R. N.; Marder, T. B. *Angew. Chem., Int. Ed.* **2006**, *45*, 489. (g) Chotana, G. A.; Rak, M. A.; Smith, M. R., III *J. Am. Chem. Soc.* **2005**, *127*, 10539. (h) Hartwig, J. F.; Cook, K. S.; Hapke, M.; Incarvito, C. D.; Fan, Y.; Webster, C. E.; Hall, M. B. *J. Am. Chem. Soc.* **2005**, *127*, 2538. (i) Coventry, D. N.; Batsanov, A. S.; Goeta, A. E.; Howard, J. A. K.; Marder, T. B.; Perutz, R. N. *Chem. Commun.* **2005**, 2172. (j) Ishiyama, T.; Nobuta, Y.; Hartwig, J. F.; Miyaura, N. *Chem. Commun.* **2003**, 2924.

(5) (a) Braun, T.; Salomon, M. A.; Altenhoner, K.; Teltewskoi, M.; Hinze, S. *Angew. Chem., Int. Ed.* **2009**, *48*, 1818. (b) Teltewskoi, M.; Panetier, J. A.; Macgregor, S. A.; Braun, T. *Angew. Chem., Int. Ed.* **2010**, *49*, 3947.

(6) Habereder, T.; Noeth, H. *Appl. Organomet. Chem.* **2003**, *17*, 525.

(7) Sagawa, T.; Asano, Y.; Ozawa, F. *Organometallics* **2002**, *21*, 5879.

(8) Suginome, M.; Nakamura, H.; Ito, Y. *Chem. Commun* **1996**, 2777.

(9) Onozawa, S.; Hatanaka, Y.; Sakakura, T.; Shimada, S.; Tanaka, M. *Organometallic* **1996**, *15*, 5450.

(10) Suginome, M.; Nakamura, H.; Ito, Y. *Angew. Chem., Int. Ed. Engl.* **1997**, *36*, 2516.

(11) Suginome, M.; Nakamura, H.; Matsuda, T.; Ito., Y. *J. Am. Chem. Soc.* **1998**, *120*, 1229.

(12) Onozawa, S.; Hatanaka, Y.; Tanaka, M. *J. Chem. Soc., Chem. Commun.* **1997**, 1229.

(13) Clegg, W.; Lawlor, F. J.; Lesley, G.; Marder, T. B.; Norman, N. C.; Orpen, A. G.; Quayle, M. J.; Rice, C. R.; Scott, A. J.; Souza, F. E. S. *J. Organomet. Chem.* **1998**, *550*, 183.

(14) (a) Curtis, D.; Lesley, M. J. G.; Norman, N. C.; Orpen, A. G.; Starbuck, J. *J. Chem. Soc., Dalton Trans.* **1999**, 1687. (b) Lesley, G.; Nguyen, P.; Taylor, N. J.; Marder, T. B.; Scott, A. J.; Clegg, W.; Norman, N. C. *Organometallics* **1996**, *15*, 5137. (c) Lu, N.; Norman, N. C.; Orpen, A. G.; Quayle, M. J.; Timms, P. L.; Whittell, G. R. *J. Chem. Soc., Dalton Trans.* **2000**, 4032. (d) Kerr, A.; Marder, T. B.; Norman, N. C.; Orpen, A. G.; Quayle, M. J.; Rice, C. R.; Timms, P. L.; Whittell, G. R. *Chem. Commun.* **1998**, 319. (e) Ishiyama, T.; Matsuda, N.; Murata, M; Ozawa, F.; Suzuki, A.; Miyaura, N. *Organometallics* **1996**, *15*, 713. (f) Clegg, W.; Johann, T. R. F.; Marder, T. B.; Norman, N. C.; Orpen, A. G.; Peakman, T. M.; Quayle, M. J.; Rice, C. R.; Scott, A. J. *J. Chem. Soc., Dalton Trans.* **1998**, 1431.

(15) Clegg, W.; Lawlor, F. J.; Lesley, G.; Marder, T. B.; Norman, N. C.; Orpen, A. G.; Quayle, M. J.; Rice, C. R.; Scott, A. J.; Souza, F. E. *J. Organomet. Chem.* **1998**, *550*, 183.
(16) Braunschweig, H.; Radacki, K.; Rais, D.; Uttinger, K. *Angew. Chem., Int. Ed.* **2006**, *45*, 162.
(17) Braunschweig, H.; Green, H.; Radacki, K.; Uttinger, K. *Dalton Trans.* **2008**, 3531.
(18) Habereder, T.; Nöth, H. *Appl. Organomet. Chem.* **2003**, *17*, 525.
(19) Braunschweig, H.; Radacki, K.; Rais, D.; Seeler, F. *Organometallics* **2004**, *23*, 5545.
(20) Braunschweig, H.; Brenner, P.; Mueller, A.; Radacki, K.; Rais, D.; Uttinger, K. *Chem.—Eur. J.* **2007**, *13*, 7171.
(21) Braunschweig, H.; Radacki, K.; Uttinger, K. *Angew. Chem., Int. Ed.* **2007**, *46*, 3979.
(22) Braunschweig, H.; Radacki, K.; Uttinger, K. *Inorg. Chem.* **2007**, *46*, 8796.
(23) Braunschweig, H.; Kupfer, T.; Radacki, K.; Schneider, A.; Seeler, F.; Uttinger, K.; Wu, H. *J. Am. Chem. Soc.* **2008**, *130*, 7974.
(24) Braunschweig, H.; Radacki, K.; Uttinger, K. *Organometallics* **2008**, *27*, 6005.
(25) Braunschweig, H.; Fuss, M.; Radacki, K.; Uttinger, K. *Z. Anorg. Allg. Chem.* **2009**, *635*, 208.
(26) Braunschweig, H.; Gruss, K.; Radacki, K.; Uttinger, K. *Eur. J. Inorg. Chem.* **2008**, 1462.
(27) Braunschweig, H.; Radacki, K.; Schneider, A. *Science* **2010**, *328*, 345.
(28) Charmant, J. P. H.; Fan, C.; Norman, N. C.; Pringle, P. G. *Dalton Trans.* **2007**, 418.
(29) Braunschweig, H.; Radacki, K.; Rais, D.; Scheschkewitz, D. *Angew. Chem., Int. Ed.* **2005**, *44*, 5651.
(30) Musaev, D. G.; Morokuma, K. *J. Phys. Chem.* **1996**, *100*, 6509.
(31) (a) Tamura, H.; Yamazaki, H.; Sato, H.; Sakaki, S. *J. Am. Chem. Soc.* **2003**, *125*, 16114. (b) Sakaki, S.; Biswas, B.; Musashi, Y.; Sugimoto, M. *J. Organomet. Chem.* **2000**, *611*, 288. (c) Sakaki, S.; Kai, S.; Sugimoto, M. *Organometallics* **1999**, *18*, 4825.
(32) Zhu, J.; Lin, Z.; Marder, T. B. *Inorg. Chem.* **2005**, *44*, 9384.
(33) Lam, W. H.; Shimada, S.; Batsanov, A. S.; Lin, Z.; Marder, T. B.; Cowan, J. A.; Howard, J. A. K.; Mason, S. A.; McIntyre, G. J. *Organometallics* **2003**, *22*, 4557.
(34) Gaspar, A. B.; Ksenofontov, V.; Seredyuk, M.; Gütlich, P. *Coord. Chem. Rev.* **2005**, *249*, 2661.
(35) Schröder, D.; Shaik, S.; Schwarz, H. *Acc. Chem. Res.* **2000**, *33*, 139.
(36) Dedieu, A. *Chem. Rev.* **2000**, *100*, 543.
(37) Poli, R. *Chem. Rev.* **1996**, *96*, 2135.
(38) Becke, A. D. *J. Chem. Phys.* **1993**, *98*, 5648.
(39) (a) Becke, A. D. *Phys. Rev.* **1988**, *A38*, 3098. (b) Lee, C.; Yang, W.; Parr, R. G. *Phys. Rev. B* **1988**, *37*, 785. (c) Miehlich, B.; Savin, A.; Stoll, H.; Preuss, H. *Chem. Phys. Lett.* **1989**, *157*, 200.
(40) (a) Frisch, M. J.; *Gaussian 03*, revision C.02; Gaussian, Inc.: Wallingford, CT, 2004. (b) Frisch, M. J.; *Gaussian 09*, revision A.01; Gaussian, Inc.: Wallingford, CT, 2009.
(41) Hay, P. J.; Wadt, W. R. *J. Chem. Phys.* **1985**, *82*, 299.
(42) (a) Couty, M.; Hall, M. B. *J. Comput. Chem.* **1996**, *17*, 1359. (b) Couty, M.; Hall, M. B. *J. Comput. Chem.* **1996**, *17*, 1359.
(43) Ehlers, A. W.; Böhme, D. S.; Gobbi, A.; Höllwarth, A.; Jonas, V.; Khler, K. F.; Stegmann, R.; Veldkamp, A.; Frenking, G. *Chem. Phys. Lett.* **1993**, *208*, 111.
(44) (a) Mennucci, B.; Tomasi, J. *J. Chem. Phys.* **1997**, *106*, 5151. (b) Cancès, M. T.; Mennucci, B.; Tomasi, J. *J. Chem. Phys.* **1997**, *107*, 3032. (c) Cossi, M.; Barone, V.; Mennucci, B.; Tomasi, J. *Chem. Phys. Lett.* **1998**, *286*, 253. (d) Tomasi, J.; Persico, M. *Chem. Rev.* **1994**, *94*, 2027.
(45) (a) Sakaki, S.; Ohnishi, Y.; Sato, H. *The Chemical Record* **2010**, *10*, 29. (b) Ishikawa, A.; Nakao, Y.; Sato, H.; Sakaki, S. *Dalton Trans.* **2010**, *39*, 3279. (c) Ishikawa, A.; Nakao, Y.; Sato, H.; Sakaki, S. *Inorg. Chem.* **2009**, *48*, 8154. (d) Ohnishi, Y.; Nakao, Y.; Sato, H.; Hiyama, T.; Sakaki, S. *Organometallics* **2009**, *28*, 2583.
(46) Mammen, M.; Shakhnovich, E. I.; Deutch, J. M.; Whitesides, G. M. *J. Org. Chem.* **1998**, *63*, 3821.
(47) (a) Braunschweig, H.; Gruss, K.; Radacki, K. *Angew. Chem., Int. Ed.* **2009**, *48*, 4239. (b) Braunschweig, H.; Gruss, K.; Radacki, K. *Inorg. Chem.* **2008**, *47*, 8595. (c) Braunschweig, H.; Gruss, K.; Radacki, K. *Angew. Chem., Int. Ed.* **2007**, *46*, 7782. (d) Braunschweig, H.; Gruss, K.; Radacki, K.; Brenner, P. *Chem. Commun.* **2010**, *46*, 913.
(48) Parameswaran, P.; Frenking, G. *J. Phys. Chem. A* **2010**, *114*, 8529.
(49) Senn, H. M.; Ziegler, T. *Organometallics* **2004**, *23*, 2980.
(50) Hayaki, S.; Yokogawa, D.; Sato, H.; Sakaki, S. *Chem. Phys. Lett.* **2008**, *458*, 329.
(51) Because of the very small energy difference between $\mathbf{TS_{3,5}}-\mathbf{Pd}$ and $\mathbf{TS_{4,5}}-\mathbf{Pd}$, we compared these two transition states with the MP4(SDQ) calculation and found that $\mathbf{TS_{3,5}}-\mathbf{Pd}$ lies higher than $\mathbf{TS_{4,5}}-\mathbf{Pd}$ by 1.4 kcal/mol, where the PCM method was employed to consider salvation effect. This energy difference is similar to that of the B3LYP calculation.
(52) Biswas, B.; Sugimoto, M.; Sakaki, S. *Organometallics* **2000**, *19*, 3895.